

An Extreme Ultraviolet Explorer Atlas of Seyfert Galaxy Light Curves: Search for Periodicity

J. P. Halpern

Department of Astronomy, Columbia University, New York, NY, 10025-6601

K. M. Leighly

*Department of Physics and Astronomy, The University of Oklahoma, 440 W. Brooks St.,
Norman, OK 73019*

H. L. Marshall

*Center for Space Research, Massachusetts Institute of Technology, 77 Massachusetts
Avenue, NE80, Cambridge, MA 02139-4307*

ABSTRACT

The Deep Survey instrument on the *Extreme Ultraviolet Explorer* satellite (*EUVE*) obtained long, nearly continuous soft X-ray light curves of 5–33 days duration for 14 Seyfert galaxies and QSOs. We present a uniform reduction of these data, which account for a total of 231 days of observation. Several of these light curves are well suited to a search for periodicity or QPOs in the range of hours to days that might be expected from dynamical processes in the inner accretion disk around $\sim 10^8 M_\odot$ black holes. Light curves and periodograms of the three longest observations show features that could be transient periods: 0.89 days in RX J0437.4–4711, 2.08 days in Ton S180, and 5.8 days in 1H 0419–577. The statistical significance of these signals is estimated using the method of Timmer & König (1995), which carefully takes into account the red-noise properties of Seyfert light curves. The result is that the signals in RX J0437.4–4711 and Ton S180 exceed 95% confidence with respect to red noise, while 1H 0419–577 is only 64% significant. These period values appear unrelated to the length of the observation, which is similar in the three cases, but they do scale roughly as the luminosity of the object, which would be expected in a dynamical scenario if luminosity scales with black hole mass.

Subject headings: galaxies: active — galaxies : Seyfert — X-rays: galaxies

1. Introduction

Some Seyfert galaxies have shown indications of transient or quasi-periodic oscillations with periods of order 1 day. The first such evidence was obtained in a 20 day *EUVE* observation of the Seyfert galaxy RX J0437.4–4711 (Halpern & Marshall 1996), where a possible signal at a period of 0.906 ± 0.018 days was detected. If attributed to relativistic beaming or other projection effects of orbiting structures at a radius of $6 GM/c^2$, a 0.9 day period requires a black hole mass of $1.7 \times 10^8 M_\odot$. Since this is the time scale on which one might expect to find periods or QPOs corresponding to orbital motion or other dynamical processes in the inner accretion disk around supermassive black holes in AGNs, it is reasonable to hypothesize that such signals may be common, and that the dearth of continuous X-ray observations of sufficient duration has prevented them from being recognized until now.

X-ray observations of AGNs that would be long enough to convincingly detect such periodic signals are rare. Although several long light curves of quasars near the ecliptic poles were obtained by the *ROSAT* All-Sky Survey, those objects did not vary during the monitoring period (Kolman et al. 1993; Treves et al. 1995). The *EXOSAT* long-look observations of Seyfert galaxies (e.g., Green, McHardy, & Lehto 1993) provided continuous light curves, but the longest was 3 days in duration so it did not adequately sample variability on time scales of ~ 1 day. There have been several analyses of possible QPO features with periods of 1 hr or less in the *EXOSAT* observations of NGC 4051 and NGC 5548 (Bao & Østgaard 1994; Papadakis & Lawrence 1993, 1995), although the NGC 5548 claim has not withstood critical analysis (Tagliaferri et al. 1996). Edelson & Nandra (1998) did not detect any periodicity in a continuous four-day observation of NGC 3516 with *RXTE*. The many “reverberation-mapping” campaigns have been longer in duration, but most were not sensitive to X-ray variability on time scales of hours to a few days. One exception is the month-long *RXTE* observation of NGC 7469 (Nandra et al. 1998), which did not, however, reveal any short-term periodicity. A possible indication of periodicity was obtained in a five-day *ASCA* observation of the Seyfert galaxy *IRAS* 18325–5926. A signal at 16 hr was seen in those data (Iwasawa et al. 1998). Lee et al. (2000) pointed to a possible 33 hr period in an 8 day observation of MCG–6–30–15 with *RXTE*. Boller et al. (2001) claimed that an 8 hr observation of Mrk 766 by *XMM-Newton* shows a period of 4200 s, although its significance according to the analysis of Benlloch et al. (2001) is not very high.

2. EUVE Observations of Seyfert Galaxies

The *EUVE* Deep Survey/Spectrometer (DS/S) telescope with Lexan/Boron filter was used for most of the pointed observations in the Guest Observer phase of the mission, from

1993 January through 2001 January. A description of the instruments on *EUVE* and their performance can be found in Sirk et al. (1997). Although the DS Lexan band is sensitive in the range 67–178 Å, photons are detected from extragalactic sources only at the short wavelength end because of the steep increase in interstellar absorption as a function of wavelength. For example Halpern, Martin, & Marshall (1996) show the effective energy distribution of detected photons in the DS for a range of power-law source spectra. Since nearly all of the detected flux is in the range 70–100 Å (0.12–0.18 keV), we refer to this band, according to convention, as soft X-rays.

It may not be well known that the *EUVE* Deep Survey imager (DS) made more long X-ray observations of Seyfert galaxies than any other X-ray satellite. *EUVE* made 23 nearly continuous observations, interrupted only by Earth occultation, of 14 Seyfert galaxies and QSOs. The duration of these pointings ranged from 3 to 33 days. In total, they account for some 231 days of elapsed time. A log of the observations presented here is given in Table 1. (We do not include in this paper many shorter *EUVE* observations of additional Seyfert galaxies that were detected in the DS.) These do not represent a complete or unbiased sample of Seyfert galaxies in any sense. Most were chosen mainly on the basis of their detectability with *EUVE*, a rare prospect whose chances are improved by selecting targets having small Galactic and intrinsic absorbing column densities. Also, famous Narrow-line Seyfert 1 Galaxies (NLS1s) are heavily represented (NGC 4051, Mrk 478, Ton S180, RE J1034+396) because they are bright, soft X-ray sources with steep X-ray spectra (Leighly 1999b).

Many of these data sets have been published, at least in part, by the authors listed in the notes to Table 1. Few of these papers, however, were concerned with power-spectrum analysis or evidence for periodicity. Several papers presented spectra of the Seyferts from the *EUVE* short-wavelength spectrometer, a heroic effort that, unfortunately, yielded results that only a mother could love. However, the corresponding long DS light curves, which are of a quality ranging from mediocre to excellent, deserve a separate and comprehensive analysis. For this paper, we simply extracted a light curve from the DS imager using a circle whose radius was chosen to include at least 95% of the source counts, and a surrounding annulus for background subtraction. Correction factors for dead-time and Primbsching (variable loss of photons when the count rate is high because of designed telemetry sharing between the instruments on *EUVE*) were also applied. These effects are discussed further in §3.2. When such a light curve is binned into one point per satellite orbit, as in Figures 1–6, it constitutes a uniformly sampled time series for which an ordinary periodogram can be calculated to search for features from 3 hours to several days.

3. Searching for Periodicity

3.1. Preliminary Requirements

It is important to explain what is meant here by “periodicity”. Since AGN power spectra are usually dominated by red noise, it is difficult to define a rigorous statistical test for periodicity, since any such feature is superposed on a continuum of power that is itself poorly characterized. Some calculations of statistical significance in the AGN literature are grossly wrong, since they are tests against the hypothesis of white noise, or worse, a constant source. Similarly, it is not possible to establish a period in a Seyfert galaxy by marking off two or three peaks in a light curve and declaring their separation to be “the period”. Accretion-powered sources flicker; the dominant feature of flickering is often an apparent variation of two or three “cycles” over the span of the observation.

We employ some simple criteria to identify plausible candidate periods. Most important, we require that there be a narrow peak or a QPO in a periodogram that 1) is clearly separated from the low-frequency noise, and 2) stands out high above the surrounding points. Some of the candidates to be reported here meet these criteria for significance, but they are not secure enough if only because the signal is not clearly present throughout the entire observation. However, theory accommodates or even favors *transient* periods in Seyfert galaxies, since orbiting hot spots or other asymmetric structures in an accretion disk *should* have finite lifetimes due to Keplerian shear. Such quasi-periods could, in principle, be confirmed by observing repeated occurrences. A third requirement is that the number of cycles detected (coherence time) should be large. One would like to see at least 10 cycles of variation to prove the existence of a period; 20 cycles would be quite convincing. These requirements (many cycles, allowing for transience) lead to an ideal observing time of 1 month to search for periodicity of order 1–2 days. Some of the light curves in Figures 1–6 show variations of order unity on 1–2 day time scales, and so are highly suited to such a search. In §4, we identify candidate periods from the periodograms of three objects, and in §5 we describe the results of the best formal analysis of statistical significance that is available for such data.

3.2. Instrumental Effects

There are no technical problems that prevent the search for periodicities of order 1 day with *EUVE*. Most of the targets were well detected, and in most cases their variability amplitudes are larger than their counting statistics, which in turn are larger than background and systematic effects. The signals to which we are sensitive would constitute a major feature of the light curve, not a subtle effect. We always take special care to apply and evaluate dead-

time and Primbsch corrections. These losses are usually due to high background radiation rates that are further enhanced in the vicinity of the South Atlantic Anomaly (SAA). We use only data obtained when the satellite is on the night side of the Earth. Most notably, the results that we describe below are not contaminated by a periodic signal at 0.99 days that can be generated by passages through the SAA, even while there is a strong modulation in the dead-time at this period. The expected values of such artificially induced periods are well known, and they are easily recognized and eliminated in a power-spectrum analysis of a long observation, as we describe below. It is fortunate that the intrinsic variability amplitude of our targets is large and reliably measured, which we have verified through analyses of additional sources in the fields of these targets that are either constant, or show uncorrelated variability (Halpern & Marshall 1996; Halpern, Martin, & Marshall 1996; Halpern et al. 1998). In summary, we have identified no instrumental or terrestrial effects that could be responsible for the candidate periods described below.

4. Results on Individual Objects

4.1. NGC 4051

NGC 4051 was the first Seyfert galaxy for which variability on time scales as short as 150 s was seen (Marshall et al. 1983). It has the lowest luminosity of the Seyfert galaxies observed by *EUVE*, and it is probably not a coincidence that it exhibits the most rapid and large-amplitude variability, in addition to extended low states in which the variability is reduced (Uttley et al. 1999). Its EUV flux was well correlated with simultaneous X-ray variations as observed by *RXTE*, with no measurable time lag. In the Comptonization model for the hard X-rays, this implies that the Comptonizing region is smaller than $20 R_{\text{Sch}}$ for $M_{\text{BH}} > 10^6 M_{\odot}$ (Uttley et al. 2000). NGC 4051 is the one object that varies too rapidly to be adequately sampled once per *EUVE* orbit, so we did not calculate a periodogram for it. A periodogram for the 1996 May observation was presented by Cagnoni et al. (1999), but it shows only features at the satellite orbital frequency and its first harmonic.

4.2. NGC 4151

Although NGC 4151 is one of the brightest Seyfert 1 galaxies in optical and X-rays, it is also highly absorbed at soft X-ray energies, so it is not surprising that it was a very weak *EUVE* source.

4.3. NGC 5548

The observation of NGC 5548 in 1998 June was conducted simultaneously with *ASCA* and *RXTE* (Chiang et al. 2000). These authors noted that, contrary to some naive expectations, the variations in the DS light curve actually seem to *lead* similar modulation at harder X-ray energies by 10–30 ks. They suggested that the EUV emission is indicative of the underlying physical variability of the source, and that the optical through EUV portion of the spectrum provides the seed photons for the production of hard X-rays via thermal Comptonization.

4.4. RX J0437.4–4711

RX J0437.4–4711 is an ordinary Seyfert 1 galaxy that was detected serendipitously in a 20 day *EUVE* observation in 1994 November and December of the millisecond pulsar PSR J0437–4715, which lies only 4′ away. A shorter observation of the same field was performed in 1994 January. The small Galactic column in this direction enhances the detectability of both objects. Results on the pulsar were published by Halpern, Martin, & Marshall (1996), and the Seyfert galaxy by Halpern & Marshall (1996), in which a possible period at 0.906 days was noted. A periodogram very similar to Figure 7a, which is based on the final archived data, appeared in the latter paper. The structure that is responsible this signal in RX J0437.4–4711 is evident in its light curve in Figure 3, especially in the second half of the observation. At least 11 cycles are present during the second half of the observation. Here, we note that the periodic signal is enhanced in the periodogram if only the second half of the observation is included (Figure 7b). The shift of the location of the peak from 0.906 days to 0.89 days when only the second half of the observation is used is within the expected range of uncertainty, $\Delta P \sim 0.2P^2/T \approx 0.016$ days, where T is the duration of the observation.

4.5. RX J0437.1–4731 and RX J0436.3–4714

These weak sources appear in the same field as RX J0437.4–4711 and PSR J0437–4715. They are also listed as unidentified, EUVE J0437-475 and EUVE J0436–472, respectively, in the Second *EUVE* Source Catalog (Bowyer et al. 1996). Armed with precise positions from the *ROSAT* High Resolution Imager, we identified both of these sources spectroscopically as NLS1s using the CTIO 1.5m telescope in 1998 October and 1999 November. Their redshifts are $z = 0.144$ for RX J0437.1–4731 and $z = 0.361$ for RX J0436.4–4714.

4.6. Ton S180

Ton S180 is a NLS1 galaxy. The 33 day *EUVE* observation of Ton S180 in late 1999 was coordinated with *ASCA* and *RXTE* during the last 12 days (Edelson et al. 2002; Turner et al. 2002). The light curves during the 12 day period of overlap are well correlated, with no apparent time delays. Leighly (1999a) showed that NLS1s are more variable than ordinary Seyfert galaxies of similar X-ray luminosity, and the *EUVE* light curves of Ton S180 (and Mrk 478, another NLS1) seem to bear this out. The 1999 *EUVE* observation of Ton S180 was the only one in our compilation to suffer significantly from imperfect correction of dead-time and Primbsching due to high background. However, the symptom of this problem is easily recognized and eliminated. When the background is high and the correction factor is $\gtrsim 2$, the correction becomes inaccurate, possibly nonlinear, and one or two orbits of data per day are clearly discrepant from the others. These bad points induce a signal in the periodogram at 0.99 days (and its harmonics), which is the period at which the SAA on the rotating Earth passes through the night side of the slowly precessing satellite orbit. (Data obtained when the satellite is on the daylight side of the Earth are not used here). When the bad points, in this case less than 10% of the data, are excised, the 0.99 day signal in the periodogram disappears. Figure 4 shows the light curve cleaned of bad points.

The periodogram of the cleaned 1999 observation of Ton S180 (Figure 8) shows several possible periods, the strongest being at 2.08 days. It is important to note that because this observation was so long, the detected period cannot be attributed to a sub-harmonic of the 0.99 day SAA period, as it is well resolved from it. Furthermore, the 2.08 day signal is much stronger than any weak residual at 0.99 days (1.18×10^{-5} Hz), the latter being undetected in the periodogram of the cleaned light curve. Weaker peaks in Figure 8 are present at 2.81 days and 1.33 days, again, with no known instrumental effect that could be responsible.

4.7. Mrk 478

The light curve of the 1993 April observation of Mrk 478 is taken directly from Marshall et al. (1996). Because part of the observation was performed with the source on the boresight position and part with the source off-axis, corrections had to be applied for the difference in effective area to produce a continuous light curve. This procedure was described in Marshall et al. (1996). That paper also showed how the spectral energy distribution of Mrk 478 peaks in the EUV.

4.8. 1H 0419–577

The *EUVE* observation of 1H 0419–577 was the second longest in this compilation, 26 days. Its periodogram, shown in Figure 9, has a peak at 5.8 days. Similar to the case of Ton S180, there may be weaker signals at other frequencies. Interestingly, 1H 0419–577 does not appear to suffer as much from the red noise that dominates RX J0437.4–4711, Ton S180, and other Seyfert galaxies at low frequencies; thus the feature at 5.8 days is more prominent. It is not clear what is responsible for this qualitatively different behavior, or indeed if it is a persistent property of the power spectrum of the source. It is possible that the 5.8 day signal simply *is* the red-noise behavior of this object, as the observation only spans ≈ 4.5 cycles of that period. This light curve of 1H 0419–577 was published without any analysis or interpretation in a paper about the serendipitous discovery of a new AM Her star only 4' from the Seyfert galaxy in this observation (Halpern et al. 1998). The latter paper illustrated that *EUVE* can reliably discover periods. In the case of the AM Her star, the period of 85.821 minutes was unambiguous despite its proximity to the satellite orbit period (96.4 minutes) because the observation was so long. This may be the only *EUVE* observation in which *two* new periods were discovered.

4.9. 3C 273

The variability amplitude of this high-luminosity QSO is small on short time scales. Note that one observation in 1994 June was badly compromised by placement of the source on a “dead spot” in the DS microchannel plate that had been created by an earlier observation of the bright EUV source HZ 43. The reduced count rate and large fluctuation during this observation (Figure 5c) is evidently due to this unfortunate placement, and should be disregarded.

4.10. E 1332+375

This QSO was discovered (Reichert et al. 1982) as a serendipitous X-ray source in an *Einstein* observation of the RS CVn type star BH CVn. It was then detected in an *EUVE* pointing at the same star (Christian et al. 1999). The small Galactic column in this direction, $N_{\text{H}} = 9.2 \times 10^{19} \text{ cm}^{-2}$, undoubtedly contributes to its detectability.

5. Formal Test for Periodicity

In this section, we attempt to quantify the statistical significance of the periodic signals seen in the periodograms of RX J0437.4–4711, Ton S180, and 1H 0419–577 in Figures 7–9. Perhaps the closest approximation to a formally correct analysis of significance is that of Timmer & König (1995), as implemented by Benlloch et al. (2001)¹. Timmer & König (1995) correctly take into account randomness in both Fourier amplitudes and phases in simulating the power spectra of flickering [$P(F) \propto f^{-1}$] or random-walk [$P(F) \propto f^{-2}$] light curves. These processes are good descriptions of many AGN power spectra which, in the range of frequencies sampled here, typically follow the form $P(F) \propto f^{-\alpha}$ where $1 < \alpha < 2$. We apply this method to estimate the statistical significance of tentative periodic signals seen in the periodograms of RX J0437.4–4711, Ton S180, and 1H 0419–577, which are the three Seyferts that *EUVE* observed for at least 20 days each in continuous or nearly continuous stretches. The approach involves simulating many red-noise light curves that match the real data in sampling time, count rate, and variance, and comparing their periodograms to the periodograms of the real data. For a discrete peak in an observed periodogram to be significant, it must have greater power than nearly all of the simulations at that frequency.

In order to determine what red-noise power-law index α matches a particular data set, we followed a procedure similar to that used by Leighly (1999a) and Done et al. (1992), and essentially the same as Uttley, McHardy, & Papadakis (2002). We simulated 100 light curves for each of a range of values of α and standard deviation σ of the light curve that are related to the integrated power spectrum of the data. Each simulated light curve was constructed as follows. We first generated a time series with 10 s time resolution that is longer by up to a factor of 2 than an actual *EUVE* light curve. For example, to simulate light curves for Ton S180 a time series of 524,288 points was required. A light curve was then drawn with random starting time from this time series, then resampled and binned exactly as the *EUVE* light curve. It was then rescaled by adding the average count rate so that Poisson noise could be added by replacing each point by one drawn from a Poisson distribution having the same number of counts. Periodograms for each of these 100 light curves were computed. These periodograms were rebinned logarithmically, and the average and standard deviation at each frequency were computed. They were then compared using χ^2 with the similarly-rebinned power spectrum from the observed light curve. The minimum in χ^2 was found as a function of α and total variance. Minimum χ^2 were obtained for $\alpha = 1.55, 1.3$, and 1.3 for RX J0437.4–4711, Ton S180, and 1H 0419–577, respectively. We note that the minima are generally fairly broad, so the range in α and σ must contribute to

¹<http://astro.uni-tuebingen.de/software/idl/aitlib/>

uncertainty in the final significance of the candidate signals.

Finally, 1,000 simulated light curves were generated for each object using its best-fitted values of α and σ of the light curve, their periodograms were generated, and the resulting exponential probability distribution of power at each frequency was calculated. Upper limits on the simulated power at various confidence levels are graphed in comparison with the actual periodograms in Figures 7–9. For example, the 99.9% confidence limit for Ton S180 is below the observed peak at 2.08 days, which means that fewer than 0.1% of the simulations had as much power at 2.08 days as is observed. In Figure 8, one can also see features in the simulations of Ton S180 near a period of 1 day and its harmonic that are caused by gaps in light curve where bad points in the observation were removed; this process has no effect on the significance of the detected signal at 2.08 days. We note that the way simulated periodograms are created for this application constitutes a conservative test in that we distribute *all* of the observed variance in the light curve among the red-noise components, whereas some of the observed variance could be due to the periodic signal that we are evaluating, if it is real.

The formal, single-trial probability for chance occurrence of the 2.08 day signal in Ton S180 is 1.6×10^{-4} . However, one must also take into account the number of independent frequencies searched and the possibility that a false signal might arise at any one of these. In the analysis of Ton S180, we searched 128 independent frequencies from $3.5 \times 10^{-7} \text{ s}^{-1}$ to $4.6 \times 10^{-5} \text{ s}^{-1}$, which is half the Nyquist frequency for a sampling interval of one satellite orbit. While there is no rigorous way of extending the single-trial significance to other frequencies that have different mean power levels, we can approximate the “global significance” of the detection in a manner similar to Benlloch et al. (2001), by multiplying the single-trial chance probability by the number of frequencies searched. In this case, the global significance becomes 98%. Similar analysis shows that the single-trial period detection is significant at 99.9% confidence for RX J0437.4–4711, but only in the second half of the observation (Figure 7b). If the entire light curve is used, the significance of its periodic signal drops to 99.7% (Figure 7a); it is clearly coming from just the second half of the observation. The global significance corresponding to Figure 7b is 96%. Period detection in 1H 0419–577 is significant at 99.6% for a single trial, but only 64% globally. Thus, we find that two of the three candidate periods have global significance $> 95\%$, a tantalizing if not entirely conclusive result.

6. Theoretical Implications

One notable pattern among the candidate periods detected here in three objects is their ordering as a function of redshift and luminosity. The flux of Ton S180 is approximately

twice that of RX J0437.4–4711, and its redshift is slightly higher. Thus, the luminosity of Ton S180 is about 2.5 times that of RX J0437.4–4711. If the luminosity of the source is proportional to the mass of the black hole, which in turn is proportional to the characteristic (dynamical) time scale, then one might expect the period of Ton S180 (2.08 days) to be about 2.5 times that of RX J0437.4–4711 (0.89 days), not far from the “observed” factor of 2.3. Also, since the fluxes detected by *EUVE* from 1H 0419–577 and RX J0437.4–4711 are approximately the same, their luminosities scale as z^2 . Then one might expect the period of 1H 0419–577 (5.8 days) to be about 4 times that of RX J0437.4–4711, not far from the “observed” factor of 6. It is encouraging that these period values appear to be related to the luminosities of the objects, a physical quantity, and not, for example, to the length of the observation, which might have favored a more prosaic explanation in terms of the frequently deceptive properties of red noise.

A striking property of these *EUVE* light curves is the large amplitude and rapid variability of some of them. Although it is generally true that variability amplitude in AGNs increases with increasing photon energy, it is now clear that EUV variability is as dramatic as any detected at higher energies. Therefore, it is of fundamental importance to measure variability in the EUV because of the likelihood that this component contains the bulk of the emission from the inner accretion disk, and most of the bolometric luminosity as well. This is certainly true in the case of RX J0437.4–4711. Because of its steep power-law spectrum of $\Gamma = 2.2 - 2.6$ as measured by *ROSAT* and *ASCA* (Halpern & Marshall 1996; Wang et al. 1998), the soft X-ray variability of RX J0437.4–4711 cannot be attributed to reprocessing of harder X-rays. The hard X-ray flux is less than that of the variable soft X-ray component. The same is true of two additional steep spectrum, highly variable objects, Ton S180 and Mrk 478 (Leighly 1999a; Marshall et al. 1996; Turner et al. 2002). Thus, we are probably viewing with *EUVE* the intrinsic variability of the innermost part of the accretion disk, the primary energy source. As hypothesized by Green, McHardy, & Lehto (1993) for the *EXOSAT* sample, the absence of a substantial electron-scattering corona, which would otherwise smooth out the intrinsic variations, may be what allows us to see large amplitude variability in the soft-spectrum EUV sources. In this picture, those objects with flat X-ray spectra are the ones that possess the Comptonizing layer which is needed to produce the hard X-ray reflection component, and which also diminishes variability if present.

Theory is in fact quite challenged to produce the large-amplitude EUV variability that we observe. Because of the energetics argument mentioned above, one cannot beg the question of the mechanism of variability, as is often done, by appealing to reprocessing of harder X-rays. “The buck stops here.” The EUV is where we must search for the the fundamental reason why AGNs vary, and it would be helpful if we had a characteristic time scale and amplitude to work with. For example, the most promising “diskoseismic” theory (Nowak

& Wagoner 1993; Nowak et al. 1997) predicts that radial g -modes will be trapped at the inner edge of a relativistic accretion disk, and that the observationally relevant frequency is $f = 714 (M_\odot/M) F(a)$ Hz where $F(a)$ ranges from 1 to 3.44 as the dimensionless black-hole angular momentum parameter a ranges from 0 to 0.998. For a $10^8 M_\odot$ black hole, the predicted period of oscillation ranges from 1.62 days for a Schwarzschild black hole to 0.47 days for a maximal Kerr black hole. This theory of accretion disk oscillations, which has been applied to Galactic black-hole binaries and AGNs (Nowak & Lehr 1998; Perez et al. 1997), is capable of generating the appropriate *periods* of a few hours to days in AGNs, but it cannot account for *amplitudes* of more than a few percent. Thus, while it even has some trouble in accounting for the variability of Galactic microquasars, the theory of accretion disk oscillations is further strained to try to explain the large X-ray variability amplitude observed in Seyfert galaxies.

Like Ton S180 and Mrk 478 above, some of the most dramatically variable X-ray sources are NLS1s. These are now well established as having steeper X-ray spectra than ordinary, broad-line Seyfert nuclei. Thus, they are ubiquitous in soft X-ray selected samples such as those of *ROSAT*. In *ROSAT* studies of selected NLS1s, Boller et al. (1997) and Brandt et al. (1999) hypothesized that relativistic beaming by orbiting asymmetries in the inner accretion disk must be partly responsible for their variability, which sometimes implies an efficiency greater than that possible for an isotropically emitting accreting source. If so, there should be at least some evidence for periodicity in their light curves if the emitting structures retain their coherence for several orbits. It is that sort of quasi-periodic signal that we may be seeing in these long *EUVE* light curves. However, we are still far from developing a physical theory for what creates such structures. It appears that theory will continue to lag behind observation in this field until and unless some more detailed pattern to the observations emerges.

7. Conclusions

The foundation of the supermassive black hole model for AGNs rests squarely on their rapid X-ray variability, which establishes the compact nature of these luminous objects beyond a reasonable doubt. Although AGN variability has been *exploited* for various purposes, we have barely begun to address *how* and *why* AGNs vary. The numerous “reverberation mapping” campaigns have not, as a by-product, shed much light on this question. Simultaneous, multiwavelength monitoring has cast a pall over the whole enterprise, because it has become apparent that there is no simple relation among the light curves in the various bands, e.g., the studies of NGC 7469 (Nandra et al. 1998) and NGC 3516 (Edelson et al. 2000).

In NGC 5548, there is some evidence that the underlying variability process is displayed in the EUV (Chiang et al. 2000). This might be true generally for Seyfert nuclei in which the peak of the spectral energy distribution is in the EUV, but we still don’t know how to interpret that variability. A fundamental obstacle to understanding is the apparent lack of a characteristic time scale, a period or quasi-period that could be interpreted in terms of a dynamical or other effect related to the size of the putative inner accretion disk and the mass of the black hole. It is difficult to interpret the aperiodic variability that is characteristic of all accretion-powered objects including AGNs. But if X-ray periods or quasi-periods could be found in just a few AGNs, they would provide a quantitative reference point for theory, just as QPOs in Galactic X-ray transients do for stellar-mass black holes.

The lack of any confirmed X-ray periods in AGNs might be taken as evidence that they don’t exist. On the other hand, the tentative detections reported here suggest that we may not yet have observed sufficiently on the required time scales. All three *EUVE* observations that were 20 days or more in duration show some indication of periodic behavior. Evidence is mounting that a dedicated search for periodic phenomena in Seyfert galaxies could be productive. However, unless this goal is considered worthy of another small, specialized mission, it is unlikely that the door that *EUVE* left ajar to new discoveries in this field will be re-entered in the near future.

This work was supported by NASA ADP grant NAG 5-9094 to JPH. Much of the data presented in this paper were obtained from the Multimission Archive at the Space Telescope Science Institute (MAST). STScI is operated by the Association of Universities for Research in Astronomy, Inc., under NASA contract NAS5-26555. Support for MAST for non-HST data is provided by the NASA Office of Space Science via grant NAG5-7584 and by other grants and contracts. We thank the entire staff of the Center for Extreme-Ultraviolet Astrophysics, whose dedicated operation of the *EUVE* satellite and careful processing of the resulting data motivated and enabled us to produce this Atlas. We also thank the referee for insightful comments, which led to significant improvements in this paper.

REFERENCES

- Bao, G., & Østgaard, E. 1994, *ApJ*, 422, L51
- Benlloch, S., Wilms, J., Edelson, R., Yaqoob, T., & Staubert, R. 2001, *ApJ*, 562, L121
- Boller, Th., Brandt, W. N., Fabian, A. C., & Fink, H. 1997, *MNRAS*, 289, 393

- Boller, Th., Keil, R., Trümper, J., O’Brien, P. T., Reeves, J., & Page, M. 2001, *A&A*, 365, L146
- Bowyer, S., Lampton, M., Lewis, J., Wu, X., Jelinsky, P., & Malina, R. F. 1996, *ApJS*, 102, 129
- Brandt, W. N., Boller, Th., Fabian, A. C., & Ruszkowski, M. 1999, *MNRAS*, 303, L53
- Cagnoni, I., Fruscione, A., McHardy, I. M., & Papadakis, I. E. 1999, *MmSAI*, 70, 29
- Chiang, J., Reynolds, C. S., Blaes, O. M., Nowak, M., A., Murray, N., Madejski, G., Marshall, H. L., & Magdziarz, P. 2000, *ApJ*, 528, 292
- Christian, D. J., Craig, N., Cahill, W., Roberts, B., & Malina, R. F. 1999, *AJ*, 117, 2466
- Done, C., Madejski, G. M., Mushotzky, R. F., Turner, T. J., Koyama, K., & Kunieda, H. 1992, *ApJ*, 400, 138
- Edelson, R., & Nandra, K. 1998, *ApJ*, 514, 682
- Edelson, R., Turner, T. J., Pounds, K., Vaughan, S., Markowitz, A., Marshall, H., Dobbie, P., Warwick, R. 2002, *ApJ*, 568, 610
- Edelson, R., et al. 2000, *ApJ*, 534, 180
- Green, A. R., McHardy, I. M., & Lehto, H. J. 1993, *MNRAS*, 265, 664
- Halpern, J. P., Leighly, K. M., Marshall, H. L., Eracleous, M., & Storchi-Bergmann, T. 1998, *P.A.S.P.*, 110, 1394
- Halpern, J. P., & Marshall, H. L. 1996, *ApJ*, 464, 760
- Halpern, J. P., Martin, C., & Marshall, H. L. 1996, *ApJ*, 462, 908
- Hwang, C.-Y., & Bowyer, S. 1997, *ApJ*, 475, 552
- Iwasawa, K., Fabian, A. C., Brandt, W. N., Kunieda, H., Misaki, K., Terashima, Y., & Reynolds, C. S. 1998, *MNRAS*, 295, 20
- Kaastra, J. S., Roos, N., & Mewe, R. 1995, *A&A*, 300, 25
- Kolman, M., Halpern, J. P., Shrader, C. R., Filippenko, A. V., Fink, H. H., & Schaeidt, S. G. 1993, *ApJ*, 402, 514

- Lee, J. C., Fabian, A. C., Reynolds, C. S., Brandt, W. N., & Iwasawa, K. 2000, MNRAS, 318, 857
- Leighly, K. M. 1999a, ApJS, 125, 297
- . 1999b, ApJS, 125, 317
- Marshall, F. E., Holt, S. S., Mushotzky, R. F., & Becker, R. H. 1983, ApJ, 269, L31
- Marshall, H. L., Carone, T. E., Shull, J. M., Malkan, M. A., & Elvis, M. 1996, ApJ, 457, 169
- Marshall, H. L., et al. 1997, ApJ, 479, 231
- Nandra, K., et al. 1998, ApJ, 505, 594
- Nowak, M. A., & Lehr, D. E. 1998, in Theory of Black Hole Accretion Disks, eds. M. A. Abramowicz, G. Björnsson, & J. E. Pringle (Cambridge: Cambridge University Press), 233
- Nowak, M. A., & Wagoner, R. V. 1993, ApJ, 418
- Nowak, M. A., Wagoner, R. V., Begelman, M. C., & Lehr, D. E. 1997, ApJ, 477, L91
- Papadakis, I. E., & Lawrence, A. 1993, Nature, 361, 250
- . 1995, MNRAS, 272, 161
- Perez, C. A., Silbergleit, S., Wagoner, R. V., & Lehr, D. E. 1997, ApJ, 476, 589
- Puchnarewicz, E. M., Mason, K. O., Siemiginowska, A., Fruscione, A., Comastri, A., Fiore, F., & Cagnoni, I. 2001, MNRAS, 550, 644
- Ramos, E., Kafatos, M., Fruscione, A., Bruhweiler, F. C., McHardy, I. M., Hartman, R. C., Titarchuk, L. G., & Montigny, C. 1997, ApJ, 482, 167
- Reichert, G. A., Mason, K. O., Thorstensen, J. R., & Bowyer, S. 1982, ApJ, 260, 437
- Sirk, M. M., Vallerga, J. V., Finley, D. S., Jelinsky, P., & Malina, R. F. 1997, ApJS, 110, 347
- Tagliaferri, G., Bao, G., Israel, G. L., Stella, L., & Treves, A. 1996, ApJ, 465, 181
- Timmer, J., & König, M. 1995, A&A, 300, 707
- Treves, A., et al. 1995, ApJ, 442, 589

Turner, T. J., et al. 2002, ApJ, 568, 120

Uttley, P., McHardy, I. M., Papadakis, I. E., Guainazzi, M., & Fruscione, A. 1999, MNRAS, 307, L6

Uttley, P., McHardy, I. M., Papadakis, I. E., Cagnoni, I., & Fruscione, A. 2000, MNRAS, 312, 880

Uttley, P., McHardy, I. M., & Papadakis, I. E. 2002, MNRAS, 332, 231

Wang, T., Otani, C., Cappi, M., Leighly, K. M., Brinkmann, W., & Matsuoka, M. 1998, MNRAS, 293, 397

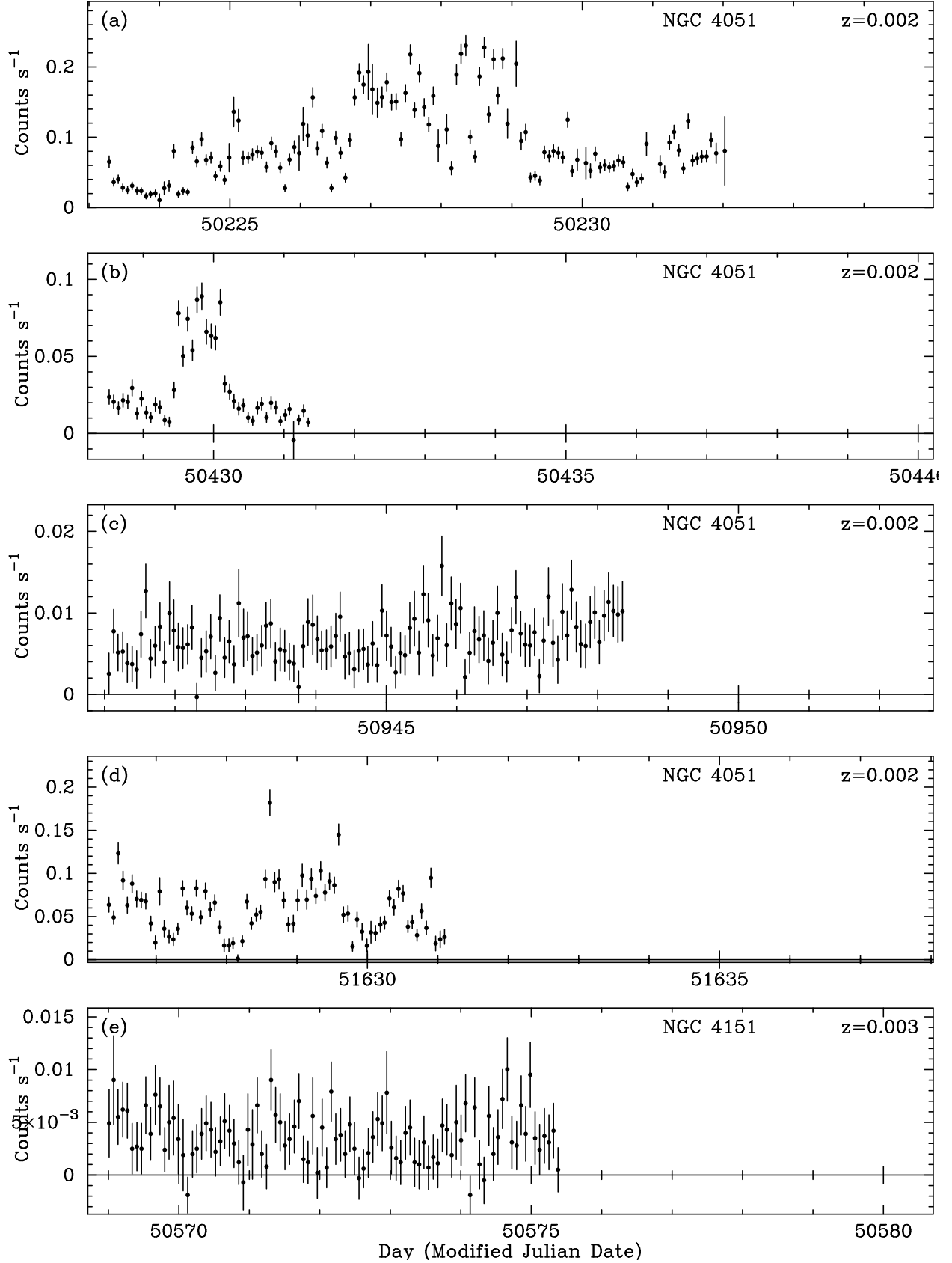


Fig. 1.— *EUVE* DS light curves of Seyfert galaxies. Each point represents one satellite orbit. Background has been subtracted, and count rates are corrected for dead-time and telemetry sharing.

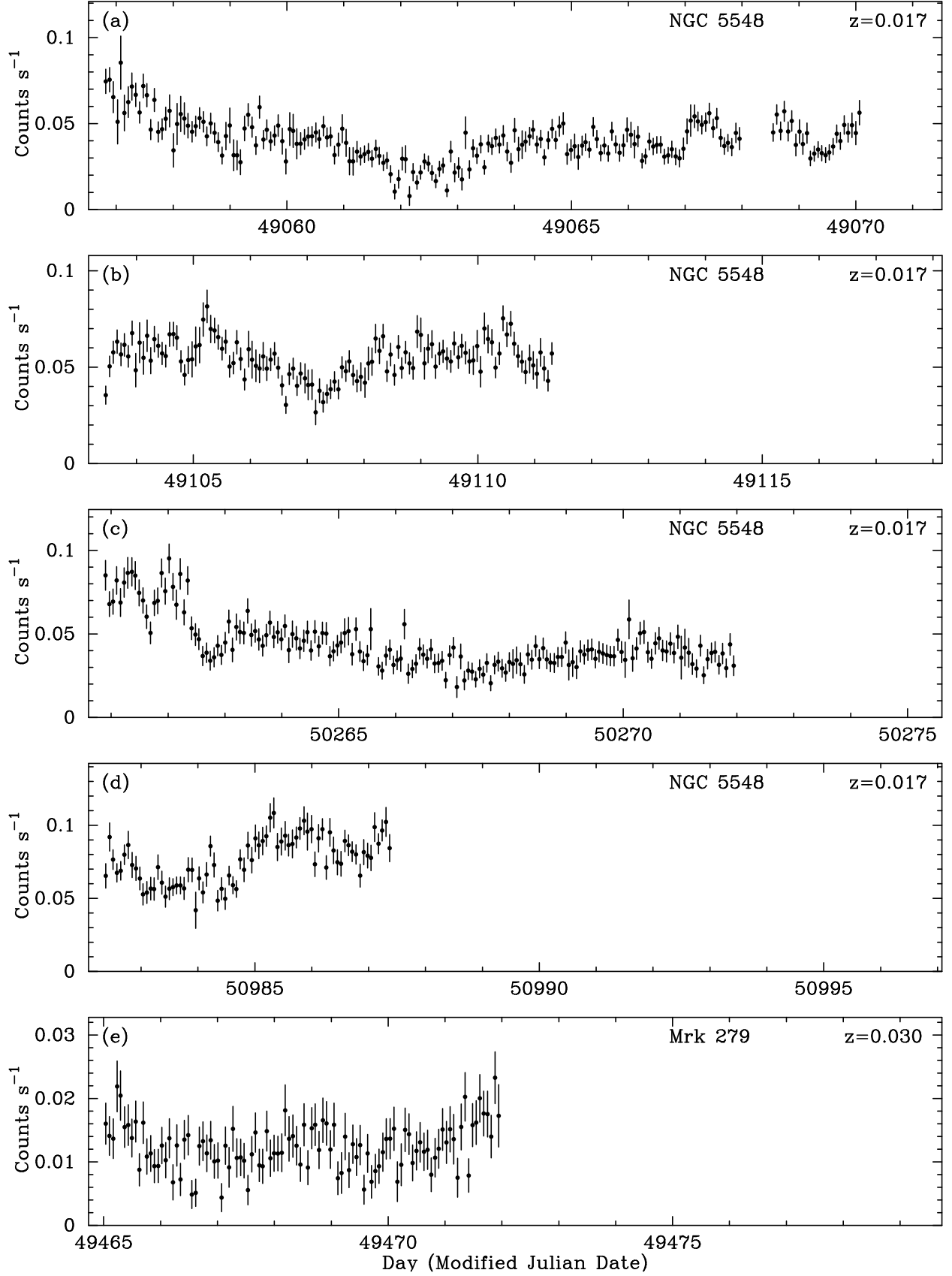


Fig. 2.— Same as Figure 1.

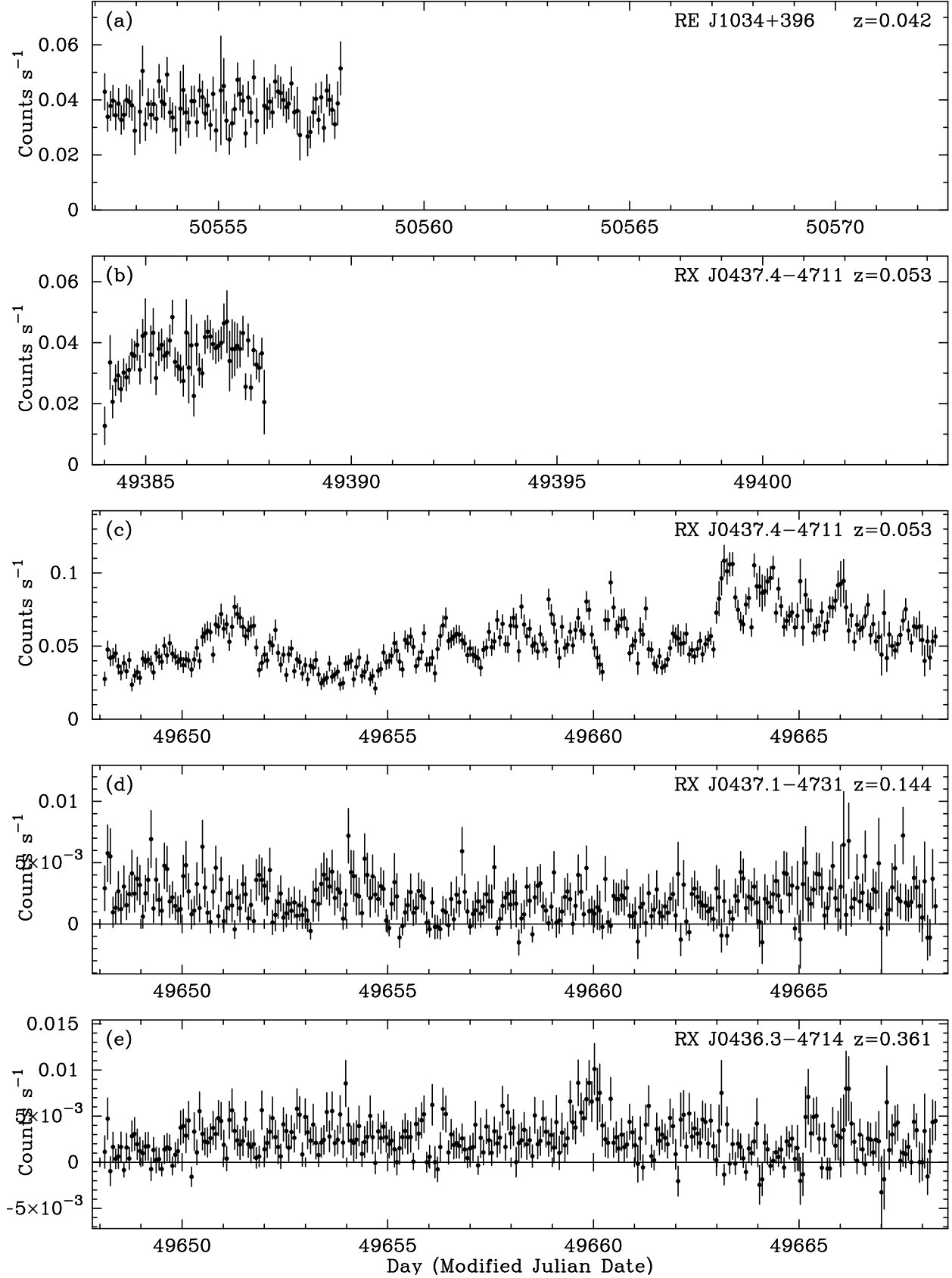


Fig. 3.— Same as Figure 1.

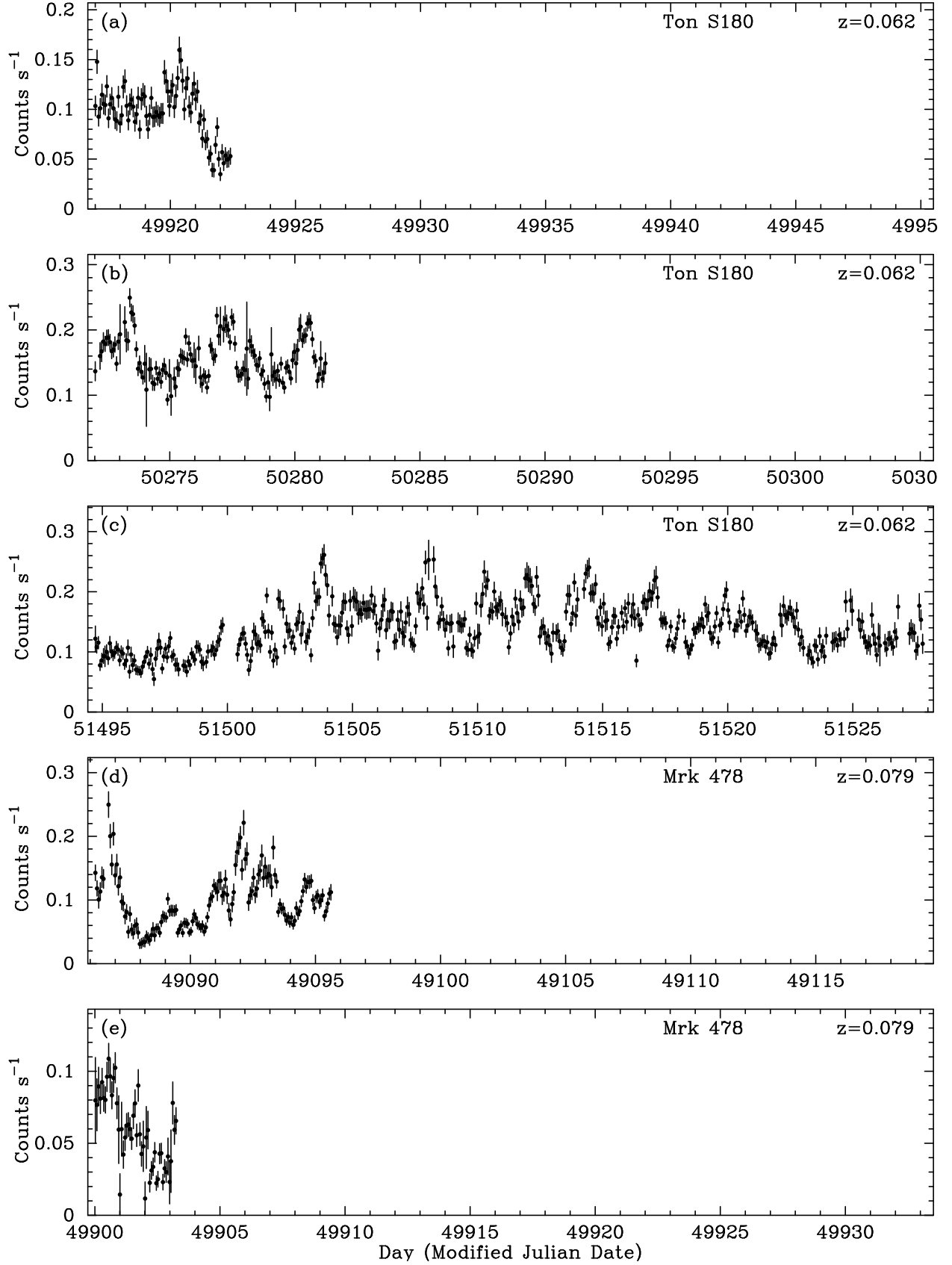


Fig. 4.— Same as Figure 1.

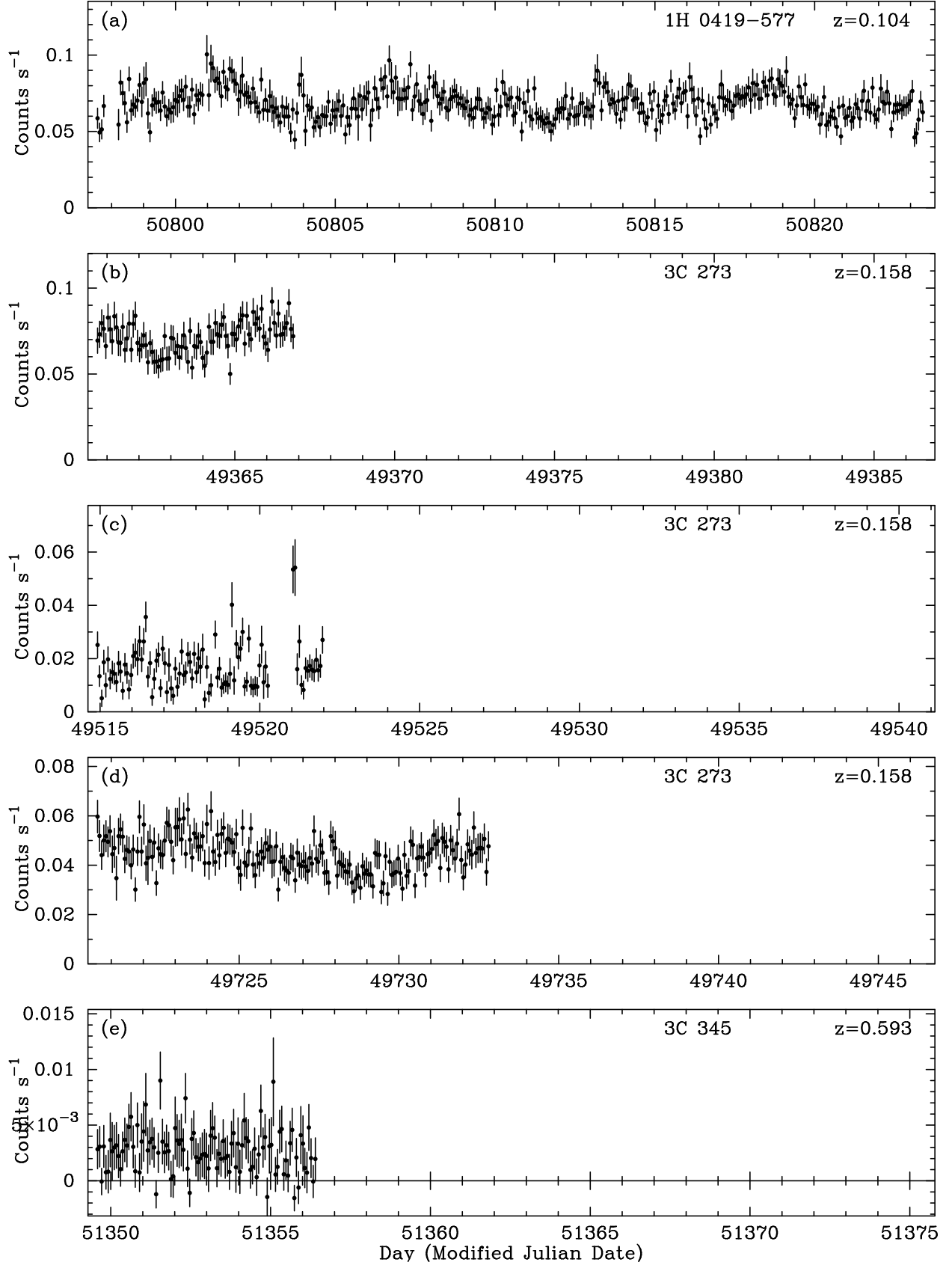


Fig. 5.— Same as Figure 1.

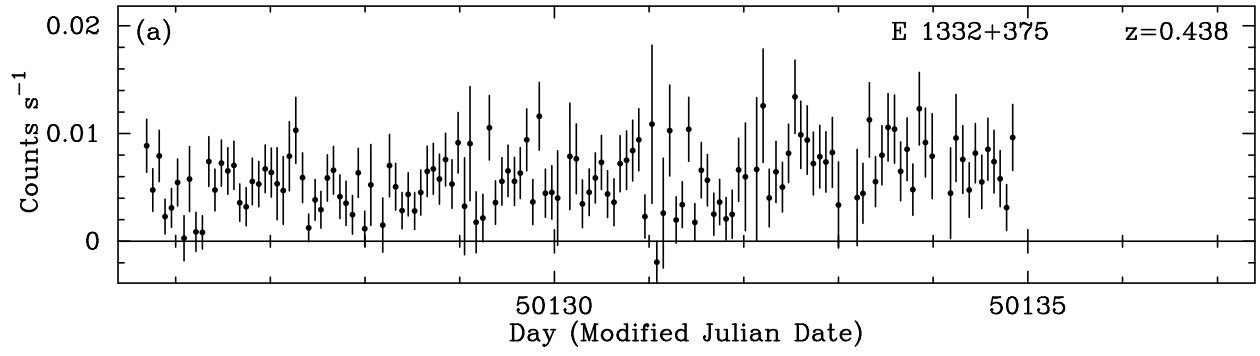


Fig. 6.— Same as Figure 1.

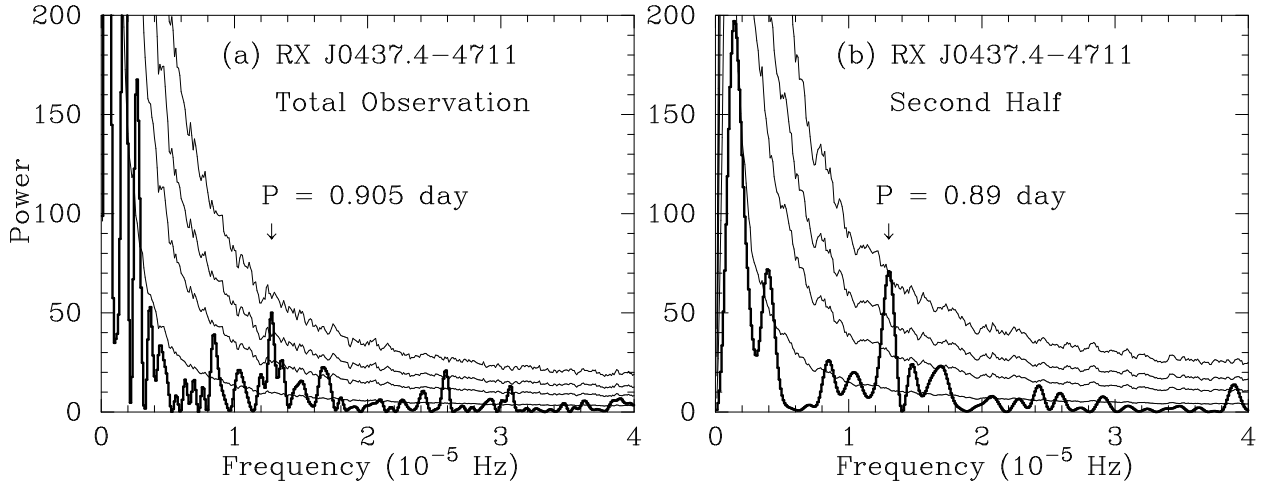


Fig. 7.— (a) Periodogram of the entire 20 day DS light curve of RX J0437.4-4711, from Halpern & Marshall (1996) (*dark line*). A possible signal at 0.906 days is marked. (b) Periodogram of the second half of the observation, showing enhanced significance of the signal, now peaking at 0.89 days. In both panels, light lines are the significance levels calculated from 1,000 simulated periodograms as described in the text. From bottom to top, the lines represent 68%, 95%, 99%, and 99.9% significance for a signal that exceeds that level of power.

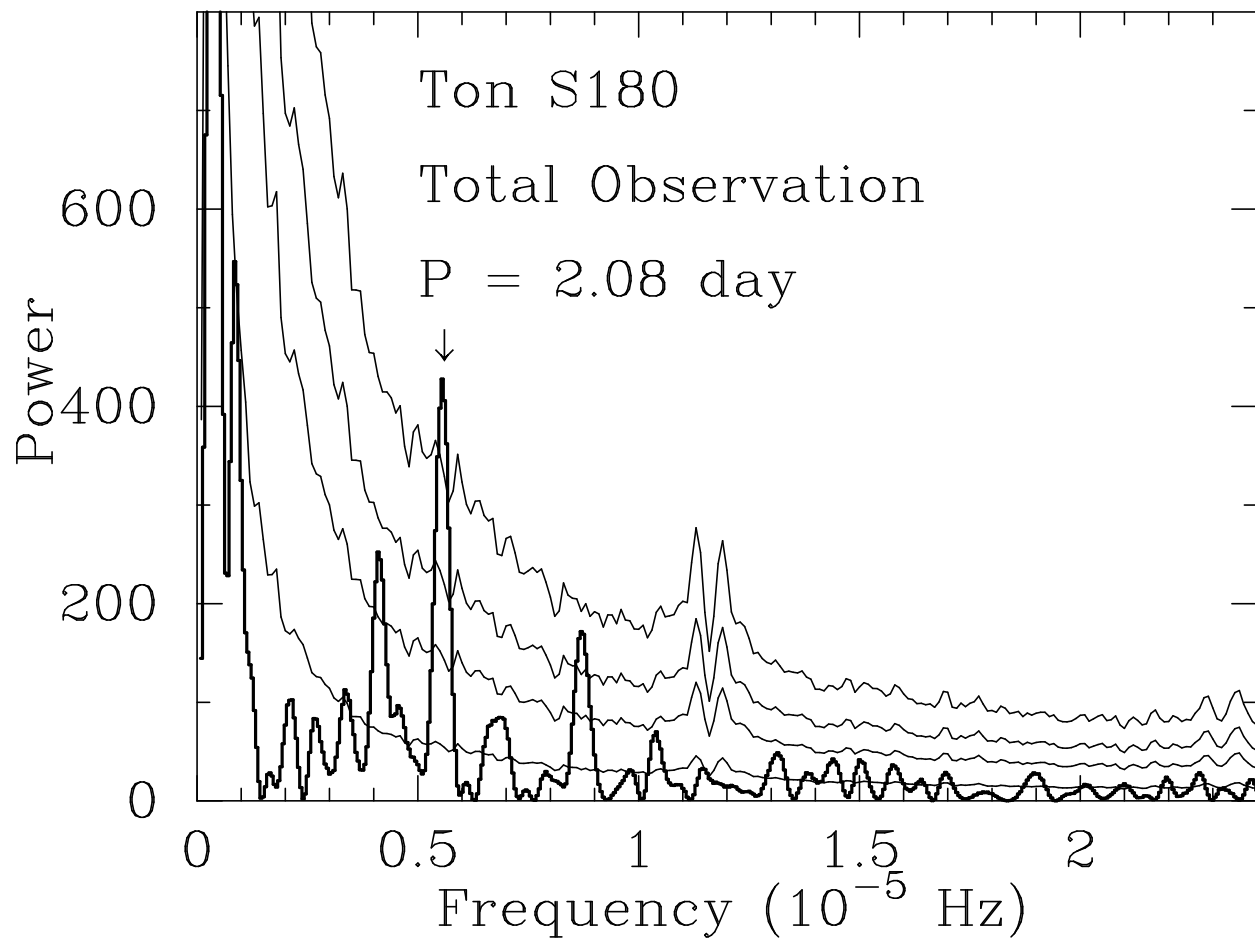


Fig. 8.— Periodogram of the long *EUVE* DS light curve of Ton S180 in 1999 Nov–Dec. Lines have the same meaning as in Figure 7.

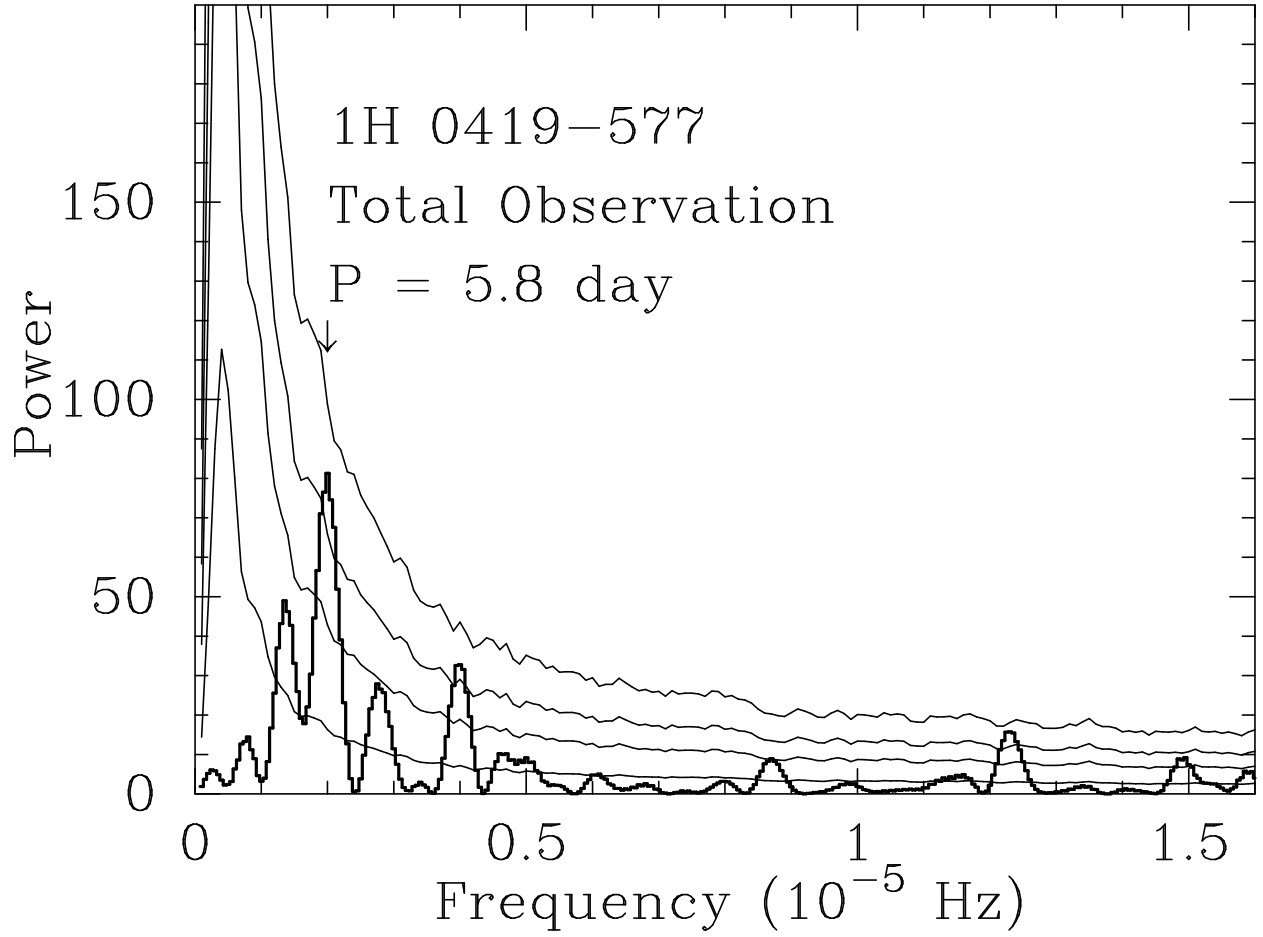


Fig. 9.— Periodogram of the *EUVE* DS light curve of 1H 0419–577. Lines have the same meaning as in Figure 7.

Table 1. Log of Observations

Object	z	Type	Dates	MJD	Figure	References
NGC 4051	0.002	NLS1	1996 May 20–29	50223–50232	1a	1,2
NGC 4051	0.002	NLS1	1996 Dec 11–14	50428–50431	1b	1,2
NGC 4051	0.002	NLS1	1998 May 8–15	50941–50948	1c	3
NGC 4051	0.002	NLS1	2000 March 23–28	51626–51631	1d	
NGC 4151	0.003	Sy1.5	1997 Apr 30 – May 7	50568–50575	1e	
NGC 5548	0.017	Sy1	1993 Mar 10–24	49056–49070	2a	4,5
NGC 5548	0.017	Sy1	1993 Apr 26 – May 4	49103–49111	2b	4,5
NGC 5548	0.017	Sy1	1996 Jun 26 – Jul 7	50260–50271	2c	
NGC 5548	0.017	Sy1	1998 Jun 18–23	50982–50987	2d	6
Mrk 279	0.030	Sy1	1994 Apr 22 – Apr 29	49464–49471	2e	7
RE J1034+396	0.042	NLS1	1994 Apr 14–20	50552–50558	3a	8
RX J0437.4–4711	0.053	Sy1	1994 Jan 31 – Feb 4	49383–49387	3b	
RX J0437.4–4711	0.053	Sy1	1994 Oct 23 – Nov 12	49648–49668	3c	9
RX J0437.1–4731	0.144	NLS1	1994 Oct 23 – Nov 12	49648–49668	3d	
RX J0436.3–4714	0.361	NLS1	1994 Oct 23 – Nov 12	49648–49668	3e	
Ton S180	0.062	NLS1	1995 Jul 18–24	49916–49922	4a	7
Ton S180	0.062	NLS1	1996 Jul 8–17	50271–50281	4b	
Ton S180	0.062	NLS1	1999 Nov 12 – Dec 15	51494–51527	4c	10,11
Mrk 478	0.079	NLS1	1993 Apr 9–18	49086–49095	4d	7,12
Mrk 478	0.079	NLS1	1995 Jul 2–5	49900–49903	4e	
1H 0419–577	0.104	Sy1	1997 Dec 15 – 1998 Jan 10	50797–50823	5a	13
3C 273	0.158	QSO	1994 Jan 8–14	49360–49366	5b	14
3C 273	0.158	QSO	1994 Jun 11–18	49514–49521	5c	
3C 273	0.158	QSO	1995 Jan 3–15	49720–49732	5d	14
3C 345	0.593	QSO	1999 Jun 20–27	51349–51356	5e	
E 1332+375	0.438	QSO	1996 Feb 12–21	50125–50134	6a	15

REFERENCES.—(1)Uttley et al. 2000;(2)Cagnoni et al. 1999;(3)Uttley et al. 1999;(4)Kaastra et al. 1995;
(5)Marshall et al. 1997;(6)Chiang et al. 2000;(7)Hwang & Bowyer 1997;(8)Puchnarewicz et al. 2001;
(9)Halpern & Marshall 1996;(10)Turner et al. 2002;(11)Edelson et al. 2002;(12)Marshall et al. 1996;
(13)Halpern et al. 1998;(14)Ramos et al. 1997;(15)Christian et al. 1999.